# Paper VII

## SPUDT filters for the 2.45 GHz ISM band

S. Lehtonen, V. P. Plessky,
C. S. Hartmann, and M. M. Salomaa



VII

# SPUDT filters for the 2.45 GHz ISM band

Saku Lehtonen, Victor P. Plessky, *Senior Member, IEEE*, Clinton S. Hartmann, *Member, IEEE*, and Martti M. Salomaa, *Member, IEEE*

*Abstract*— **Filters based on employing single-phase unidirectional transducers (SPUDTs) consisting of $\lambda/4$ and wider electrodes are presented. The design variants exploit the significant difference between the reflectivity of short-circuited $\lambda/4$ electrodes and that of floating wide electrodes on 128° $LiNbO_3$. The SAW devices operating at 2.45 GHz have critical dimensions of about 0.3–0.4 $\mu$m, accessible to standard optical lithography. When matched, the fabricated SPUDT filters exhibit minimum insertion losses of 5.5–7.9 dB together with 3 dB passbands of 89–102 MHz. The majority of the insertion loss can be attributed to the attenuation on free surface and inside the grating, and to the resistivity of the electrodes.**

## I. Introduction

Wireless communication has become a field of worldwide business with exceedingly high commercial interest. The solutions formerly developed for high-end niche applications have impinged in various customer products and services. Along with the development of technologies, the growth of businesses and subscriber numbers, the transmitting capacity, characterized by, *e.g.*, the frequency bandwidth and signal power, has become an important issue. The frequency spectrum is allocated for new standards before systems operating according to their regulations emerge. Different continents have different existing standards and systems which renders the introduction of global systems difficult. When the range of the system envisaged is short, one possibility is to pursue operation in the bands allocated for industrial, scientific and medical (ISM) purposes.

Wireless radio-frequency (RF) identification (ID) has attained plenty of attention recently. The optical readout systems have the advantages of low cost, widespread use and established status but they require unrestricted line-of-sight and proper alignment. Even though they undoubtedly will persist, their shortcomings call for more flexible systems. Various approaches for the replacement of bar codes and the improvement of logistics management in target applications are being developed. One of the proposed solutions is a global surface-acoustic wave (SAW) ID tag system operating in the 2.45 GHz ISM band [2].

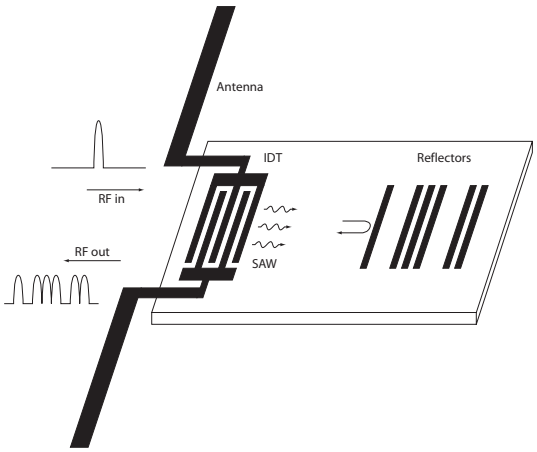


Fig. 1. Schematic of a SAW ID tag after Ref. [1].

An ID tag requires a facility to modify the incoming RF signal using a preprogrammed code and an antenna for receiving the interrogation signal and for transmitting the response. An ID tag may be passive or it may contain active components, in which case the power needed for biasing has to be supplied to the tag either by a battery or by the interrogation signal. A SAW ID tag consists of a transducer connected to the antenna, and a number of reflectors placed on the propagation part of the transmitted acoustic wave, see Fig. 1. The advantage of SAW ID tags is that the device is passive, an advantage for power budget and range. Furthermore, the device is rugged and compact. The signal picked up by the antenna is converted in a transducer into a SAW which propagates on the substrate, is reflected from tailored ID structures and reconverted by the same transducer into an electric signal and, finally, retransmitted by the same antenna.

Due to the diffraction, a SAW ID tag needs a wide

S. Lehtonen (e-mail: saku@focus.hut.fi) and M. M. Salomaa (e-mail: Martti.Salomaa@hut.fi) are with the Materials Physics Laboratory, Helsinki University of Technology, P.O. Box 2200 (Technical Physics), FIN-02015 HUT, Finland.

V. P. Plessky is with GVR Trade SA, Rue du Château 9 C, CH-2022 Bevaix, Switzerland (e-mail: victor.plessky@bluewin.ch).

C. S. Hartmann is with RF SAW Inc., 900 Alpha Drive, Suite 400, Richardson, TX 75081, USA (e-mail: chartmann@rfsaw.com).

aperture. In order to maximise the range of the system, the tag must exhibit as low losses as possible. To comply with these requirements, single-phase unidirectional transducers (SPUDTs) [3], transceiving the acoustic energy predominantly in one direction on the crystal surface, are often used. A further requirement is that the transducer structure should be feasibly manufacturable in large quantities. The majority of SPUDT approaches utilize structures where the critical dimension is on the order of 1/8 of the acoustical wavelength ($\lambda_0$). This is a severe limitation for the high-frequency operation. Since the SAW velocity is typically 3-4 km/s, a $\lambda_0/8$-wide distance at 2.45 GHz equals 0.15–0.2 $\mu$m, which is inaccessible to standard optical lithography. Some SPUDT configurations achieving wider critical dimensions have been envisaged [4, 5].

A novel SPUDT principle employing $\lambda_0/4$ and wider electrodes was recently proposed [6]. Here, the applicability of the structure and its variants is demonstrated for SPUDT filters consisting of two SPUDT transducers aligned in the same acoustic channel with their forward directions opposite to each other. Preliminary results of this work were reported in Ref. [7].

## II. SPUDT structures

In this work, SPUDT structures introduced in Ref. [6] are employed as transducers in simple filter structures. The unit cell in the basic structure of Fig. 2, reproduced from [6], comprises a pair of $\lambda/4$-wide transducer electrodes and a floating $\lambda/2$-wide reflector electrode on 128° $LiNbO_3$. The unidirectional operation of the structure is based on the considerable difference in reflectivity between the weakly reflecting narrow short-circuited electrodes and the wide floating electrodes with high reflectivity [8]. In Fig. 2, the forward direction is to the right. The great advantage of the critical dimension of $\lambda/4$, is that the structures are feasibly fabricated with standard optical lithography for frequencies up to 2.5–3 GHz.

The unit cell of this basic structure, referred to in what follows as type B, is $2\lambda_0 = 4p_0$ wide. It incorporates one center of reflection, placed roughly at the center of the reflecting electrode, and one center of excitation, located in the middle of the gap between the transducer electrodes. The difference in reflectivity is maximized by selecting the widths of the reflector and transducer electrodes as $a/p_0 = 0.8$ and $b/p_0 = 0.4$, respectively [8]. However, the structure is quite sparse, which serves to reduce its efficiency in terms of the electromechanical

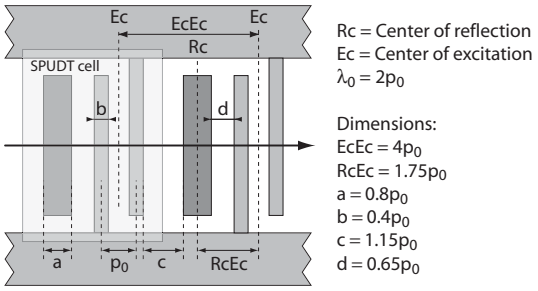


Fig. 2. Geometry of the basic SPUDT element (B). The unit cell B consists of a floating reflector electrodes ($a/p_0 = 0.8$) and a pair of narrow transducer electrodes ($b/p_0 = 0.4$). The length of the section is $2\lambda_0$.

coupling and reflectivity per wavelength. Therefore, more efficient variants where the reflectivity of a single floating reflector is compromized are proposed. The requirement of manufacturability prohibits the increase of the density of the structure by simultaneously increasing the length of the unit cell by one wavelength and adding floating $0.8p_0$-wide electrodes: centering such electrodes half a wavelength apart leads to a gap $0.2p_0$ wide between them. However, the numerical simulation results suggest that, for aluminium thicknesses 5–8% of $h/\lambda_0$, the reflectivity of a 2-electrode open-circuited grating is decreased by mere 1–2 %-units if the metallisation ratio is reduced from $a/p_0 = 0.8$ to $a/p_0 = 0.6$ [8]. The use of narrower reflector electrodes allows a center-to-center distance equal to $p_0$ between them. For $a/p_0 = 0.6$, the minimum gap width within the structure becomes $0.4p_0$, equal to the width of the transducer electrodes. Reducing the critical dimension for the nominal $0.5p_0$ to $0.4p_0$ only slightly limits the operation frequency feasible for standard optical lithography. For 128° $LiNbO_3$, at 2.45 GHz, the critical dimension of $0.4p_0 = 0.2\lambda_0$ roughly corresponds to 0.325 $\mu$m.

Examples of denser variants of the basic structure are illustrated in Figs. 3 and 4. Figure 3 shows a variant C where one unit cell is $3\lambda_0 = 6p_0$ wide. The unit cell C comprises three $0.4p_0$-wide transducer electrodes and two floating $0.6p_0$-wide reflector electrodes. Thus, instead of a single source of the basic variant (B), there are two excitation sources. In addition, due to the inclusion of second reflector electrode, the total reflectivity in the unit cell C is likely to be larger than that in the unit cell B. In Fig. 4, another variant, E, having a unit cell $4\lambda_0 = 8p_0$ wide, is sketched. The unit cell E encompasses four $0.4p_0$-wide transducer electrodes (implying three sources of excitation) and

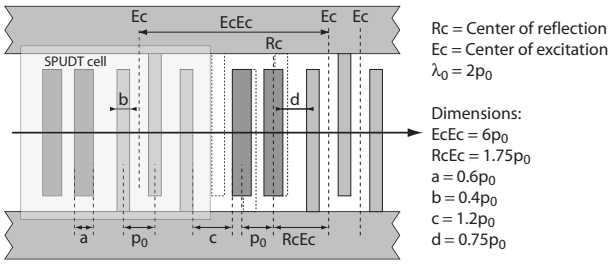


Fig. 3. Variant C of the SPUDT finger structure. The unit cell C consists of two floating reflector electrodes ($a/p_0 = 0.6$) and three narrow transducer electrodes ($b/p_0 = 0.4$). The length of the section is $3\lambda_0$. The dashed rectangles indicate the positions of transducer fingers in a synchronous structure.

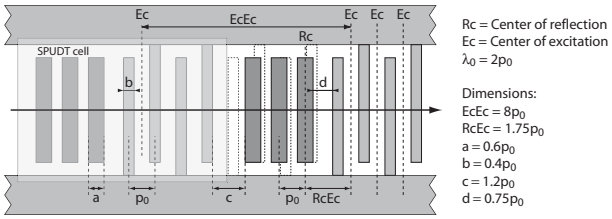


Fig. 4. Variant E of the SPUDT finger structure. The unit cell E consists of three floating reflector electrodes ($a/p_0 = 0.6$) and four narrow transducer electrodes ($b/p_0 = 0.4$). The length of the section is $4\lambda_0$. The dashed rectangles indicate the positions of transducer fingers in a synchronous structure.

three $0.6p_0$-wide reflector electrodes. The variants C and E, and longer unit cells utilizing a number of $\lambda/2$-spaced fundamental-mode floating electrodes as reflectors may be regarded as elements of a group-type SPUDT structure [9].

Test devices were fabricated and their frequency characteristics were measured directly on wafer using a wafer prober and a network analyzer. Six filter variants are considered here. One SPUDT filter, labeled 9SecB, consists of two identical transducers with opposite directivities having 9 sections of type B, see Fig. 2. The filter 7SecC has transducers utilizing 7 sections of type C, see Fig. 3. The transducers of another variant, 5SecE, comprise 5 sections of type E, see Fig. 4. In all the cases, the periodicity $p_0$ and the aperture were 0.8 $\mu$m and 75 $\mu$m, respectively. The measurement results obtained in the 50-$\Omega$ system were numerically matched with parallel inductances in the input and the output and transformed to the 350-$\Omega$ impedance system. Three more filter variants exhibiting two identical acoustical tracks in parallel (2W9SecB, 2W7SecC and 2W5SecE) and manifesting matching conditions close to 150 $\Omega$ were included. The schematic of the double-aperture variant of the SPUDT structure B, used in the filter 2W9SecB, is shown in Fig. 5.

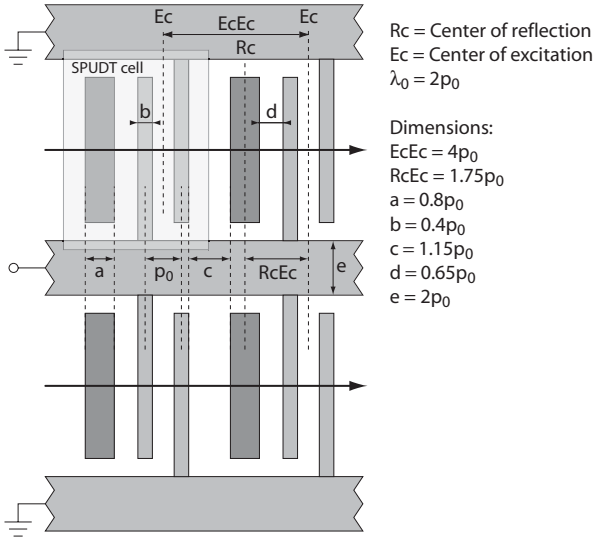


Fig. 5. Double-aperture variant of SPUDT structure B.

The filters were fabricated for the metallisation thicknesses of 5, 6.5, and 8% of $h/\lambda_0$.

## III. Experimental results

The responses of the measured SPUDT devices have been studied numerically, and partly statistically. The frequency responses measured in the 50 $\Omega$ environment are numerically matched to illustrate the optimal characteristics of the devices. Wafer-level averages and standard deviations have been evaluated for the minimum insertion loss and the 3 dB bandwidth.

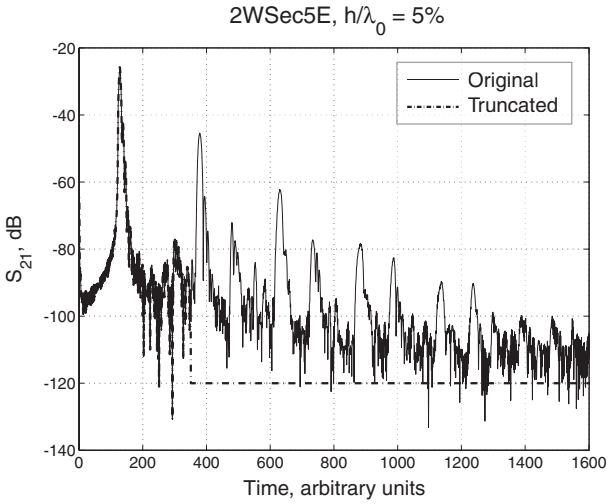


Fig. 6. Time gating used to obtain a smooth passband signal. Only one half of the response is shown.

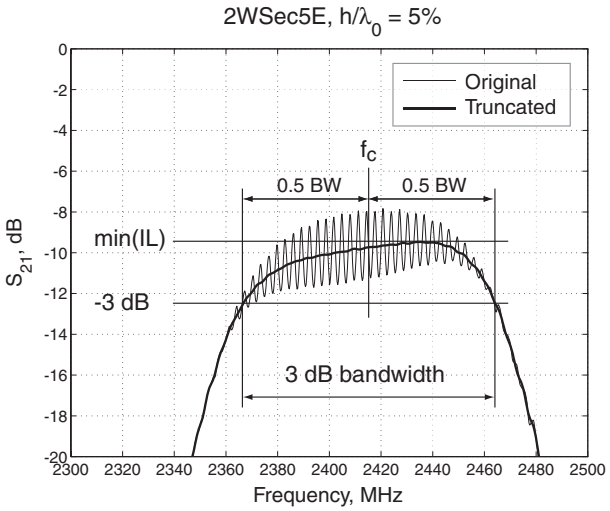


Fig. 7. Definitions of the parameters used to characterize the SPUDT filters.

Since the multiple-transit signals render the determination of the minimum insertion loss difficult, our approach is, for both matched and unmatched devices, to cut the contribution of the higher-order transit signals by time gating, see Fig. 6.

The minimum insertion loss is obtained from the smoothened response. The -3 dB frequency points and the 3 dB bandwidth are then determined, and the center frequency is taken to be the center of the 3 dB band, see Fig. 7.

The frequency response of the filter 9SecB for the thickness $h/\lambda_0 = 5\%$ is shown in Fig. 8. For the matched filter, the minimum insertion loss is 6.8 dB and the 3 dB bandwidth at 2.42 GHz is 101 MHz. Both values are wafer-level averages. For the corresponding variant with two acoustical channels in parallel (2W9SecB, Fig. 5, responses not shown), the minimum insertion loss is about 1 dB higher, and the 3 dB bandwidth is practically the same, see Table I.

The best variant in the matched environment for the thickness $h/\lambda_0 = 5\%$ seems to be the device 2WSec5E, for which the average insertion loss is 5.9 dB at the center frequency 2412 MHz. The average matched 3 dB bandwidth is 96 MHz. For the thickness 6.5%, see Fig. 9, the average insertion loss at the center frequency 2389 MHz is 5.8 dB and the 3 dB bandwidth is 104 MHz. A drawback of the slightly enhanced properties is that the device is then matched to 200 Ω instead of the 150 Ω for the lower thickness. The wafer-level averages of the characteristic values of all filter variants for the thickness $h/\lambda_0 = 5\%$ are enlisted in Table I.

In order to address losses present in the SPUDT

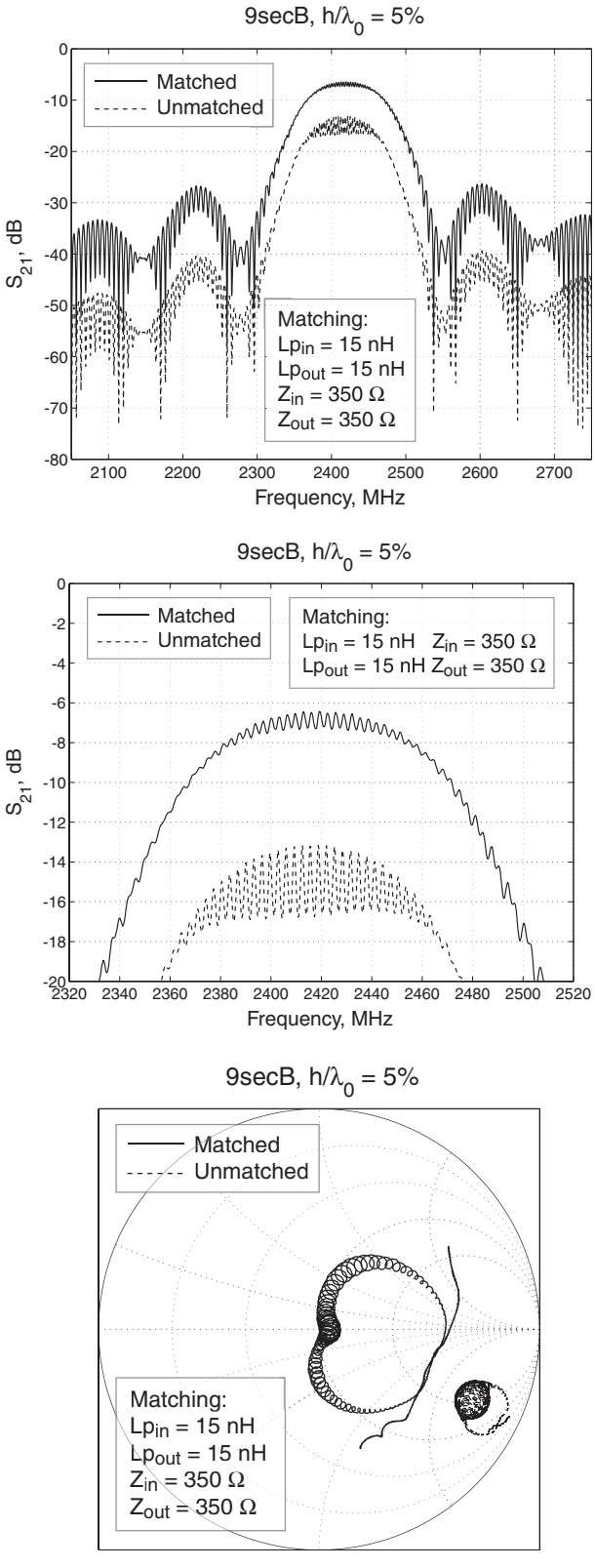


Fig. 8. Measured characteristics of the SPUDT filter 9SecB for $h/\lambda_0 = 5\%$. *Top*: Transmission response of the filter (dB). *Middle*: Detailed view of the passband. *Bottom*: $S_{11}$ on the Smith chart.

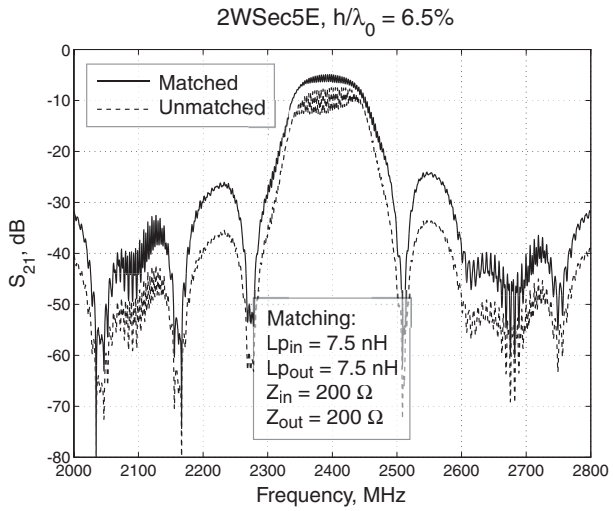


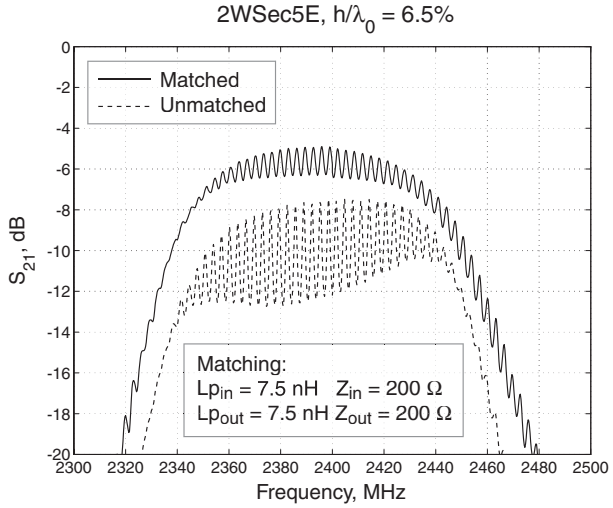


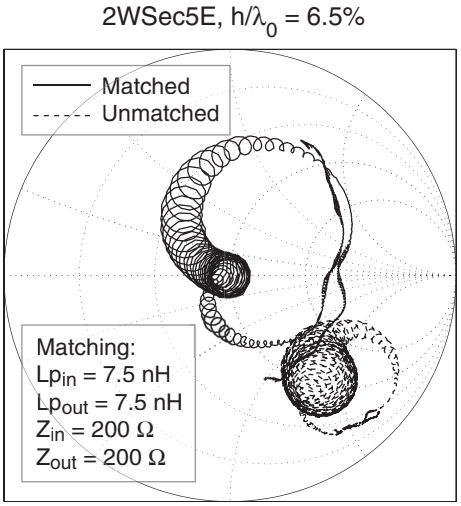


Fig. 9. Characteristics of the SPUDT filter 2WSec5E for $h/\lambda_0 = 6.5\%$. *Top*: Frequency response of the filter (in dB). *Middle*: Detailed view of the passband. *Bottom*: $S_{11}$ on the Smith chart.

TABLE I

Minimum insertion loss (matched), 3dB bandwidth (matched) and the matched impedance system for the measured devices

| Device, $h/\lambda_0 = 5\%$ | Min IL, dB (matched) | 3dB BW, MHz (matched) | $Z_m$, Ω |
|---|---|---|---|
| 9SecB | 6.8±0.1 | 101±2 | 350 |
| 2W9SecB | 7.9±2.3 | 102±4 | 150 |
| 7SecC | 5.9±0.1 | 89±2 | 350 |
| 2W7SecC | 6.8±0.9 | 90±3 | 150 |
| 5SecE | 5.5±0.2 | 95±2 | 350 |
| 2W5SecE | 5.9±0.3 | 96±3 | 150 |

structure, a simulation using a numerical tool characterizing the substrate by Green's functions and utilizing the finite element method (FEM) to describe the fields in the electrodes [10, 11] was carried out. A comparison of the experimental data to a simulated response of the structure 5SecE, imposing the same matching conditions, manifests that, in the simulations, attenuation is excluded from the Green's functions and the resisitivity of the electrodes is neglected, see Fig. 10. The losses are about 4 dB higher in the experiment than in an ideal filter consisting of 2 SPUDT transducers. The majority of the loss difference may be attributed to the propagation attenuation (on the free surface and inside the electrode structures) and to the resistivity.

The distance between the transducers (free surface) is about 600 $\mu$m, which corresponds to a delay of about 0.15 $\mu$s. Estimating the loss as 6.5 dB/$\mu$s, a value extracted from our measurement results of delay line test structures with identical IDTs and different separation betweeen them, one arrives at 1 dB of additional free-surface propagation loss. The propagation inside a metallic grating is characterized by a higher loss level. In the modelling, the attenuation parameter $\gamma \approx 3 \cdot 10^{-3}$ Nepers/$\lambda_0$ is used, corresponding at 2.4 GHz to the loss $8.68 \cdot 3 \cdot 10^{-3} \cdot 2400 = 62$ dB/$\mu$s, or to 0.026 dB/$\lambda_0$. The length of the transducer (device 5SecE) is about $20\lambda_0$. Considering the center-to-center propagation, *i.e.*, assuming the loss to arise from the propagation through half the length of each IDT, we arrive at a propagation loss on the order of 0.5 dB inside the IDTs in the device.

Attenuation in Nepers/$\lambda_0$ attributed to the resistive losses is proportional to the square of the

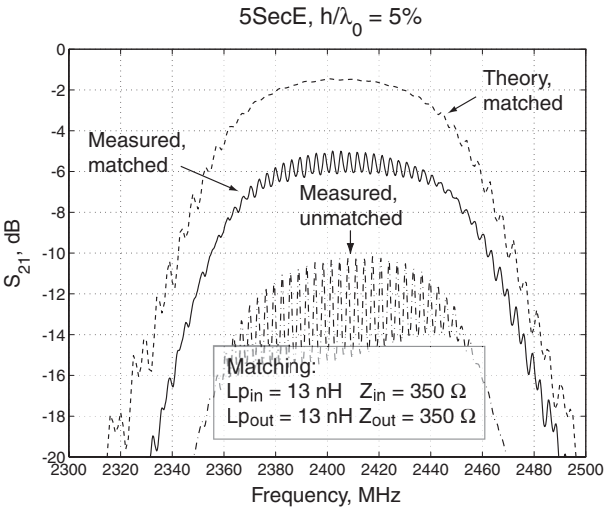


Fig. 10. Comparison of simulated and experimental frequency responses of a SPUDT transversal filter (5secE). For both transducers, $N_{\mathrm{cells(E)/IDT}} = 5$.

aperture in $\lambda_0$ [12]:

$$\gamma_{\mathrm{res}}\lambda_0 \approx 2\frac{2W}{3a}\rho_{\square}|\alpha_n|^2\frac{W}{\lambda_0} = \frac{8}{3}\frac{\rho_{\square}}{(a/p_0)}\alpha_n^2\left(\frac{W}{\lambda_0}\right)^2, \quad (1)$$

where $a$ is the finger width, $p_0 = \lambda_0/2$ is the period, and $\rho_{\square} = 0.04/h(\text{in } \mu\text{m})$ [$\Omega$] is the sheet resistivity of aluminium. The normalized coupling coefficient $\alpha_n$ is on the order of $10^{-3}(\sqrt{\Omega})^{-1}$. The metallisation ratio of the transducer fingers is $a/p_0 = 0.4$. Substituting the numerical values, we arrive at the attenuation value of 0.007 Nepers/$\lambda_0$, or 0.064 dB/$\lambda_0$, due to the resistivity. Assuming that the floating electrodes do not contribute to the resistivity, one obtains for 10 active finger pairs per transducer a total additional loss (2 SPUDTs) of 1.3 dB.

The estimated total loss due to the propagation attenuation on free surface and inside the grating and the resistivity of electrodes are 1 dB + 0.5 dB + 1.3 dB = 2.8 dB, which is less than the 4 dB obtained from the comparison of the experimental and simulated results. These estimates indicate the presence of other loss mechanisms not accounted for in the simulations.

## IV. Discussion

A novel SPUDT structure employing $\lambda/4$ and wider electrodes is proposed. The operation of the structure and its variants is based on the significant difference between the reflectivity of $\lambda/4$-wide short-circuited electrodes and that of floating wide electrodes on 128° $LiNbO_3$ [8]. SAW filters, tags, sensors and other SAW devices utilizing these unidirectional transducers, operating at 2.45 GHz, will have critical dimensions of about 0.3–0.4 $\mu$m, accessible to mass production with standard optical lithography. The fabricated SPUDT filters exhibit a relatively low insertion loss (down to 5.5 dB) and wide passband (about 100 MHz). Comparison to simulated results reveals that the majority of the losses can be attributed to attenuation on free surface and inside the grating and to the resistivity of the electrodes.

## Acknowledgements

The authors are grateful to William Steichen at Temex Microsonics SA for conferring TRANSD[1] at the disposal of HUT for this study, and, to Mr. Paul Brown for carrying out the measurements. The first author further acknowledges the Graduate School in Technical Physics for support and Helsinki University of Technology and the Foundation of Technology (Finland) for scholarships.

## References

[1] L. Reindl and W. Ruile, "Programmable Reflectors for SAW-ID-Tags", *Proc. 1993 IEEE Ultrasonics Symposium*, pp. 125-130.

[2] C. S. Hartmann, "A Global SAW ID Tag with Large Data Capacity," *Proc. 2002 IEEE Ultrasonics Symp.*, pp. 65–69.

[3] C. S. Hartmann, P. V. Wright, R. J. Kansy, and E. M. Garber, "An analysis of SAW interdigital transducers with internal reflection and the application to the design of single-phase unidirectional transducers," *Proc. 1982 IEEE Ultrasonics Symp.*, pp. 40–45.

[4] P. V. Wright, D. F. Thompson, and R. E. Chang, "Single-phase unidirectional transducers employing uniform-width dithered electrodes," *Proc. 1995 IEEE Ultrasonics Symp.*, pp. 27–32.

[5] C.-Y. Jian and S. Beaudin, "A new type SPUDT SAW for use in high frequency aroung 2 GHz," *Proc. 2002 IEEE Ultrasonics Symp.*, pp. 279–282.

[6] S. Lehtonen, V. P. Plessky, C. S. Hartmann, and M. M. Salomaa, "Unidirectional SAW Transducer for Gigahertz Frequencies," *IEEE Trans. Ultrason., Ferroelectr., Freq. Contr.*, vol. 50, No. 11, November 2003, pp. 1404–1406.

[7] S. Lehtonen, V. P. Plessky, C. S. Hartmann, and M. M. Salomaa, "Unidirectional SAW transducer for GHz frequencies," *Proc. 2003 IEEE Ultrasonics Symp.*, pp. 817–820.

[8] S. Lehtonen, V. P. Plessky, and M. M. Salomaa, "Short reflectors operating at the fundamental and second harmonics on 128° $LiNbO_3$," *IEEE Trans. Ultrason., Ferroelectr., Freq. Contr.* **51**, No. 3, March 2003, pp. 343–351.

[9] M. Lewis, "Low loss SAW devices employing single stage fabrication," *Proc. 1983 IEEE Ultrasonics Symp.*, pp. 104–108.

[10] P. Ventura, J. M. Hodé, M. Solal, J. Desbois, and J. Ribbe, "Numerical methods for SAW propagation

[1] TRANSD is a FEM/BEM-based simulator for analysis of SAWs in finite electrode structures developed by Temex Microsonics SA (Sophia-Antipolis, France) in collaboration with CMAP/Ecole Polytechnique (Paris, France).

characterization,", *Proc. 1998 IEEE Ultrasonics Symp.*, pp. 175–186.

[11] J. Ribbe, "On the coupling of integral equations and finite elements / Fourier modes for the simulation of piezoelectric surface acoustic wave components", PhD Thesis, CMAP / Ecole Polytechnique, 2002 (in French).

[12] P. V. Wright, "A New Generalized Modeling of SAW Transducers and Gratings," *Proc. 1989 IEEE Freq. Contr. Symp.*, pp. 596–605.